Characterising cross-coupling in coherent fibre bundles

PROCEEDINGS OF SPIE

SPIEDigitalLibrary.org/conference-proceedings-of-spie

Characterising cross-coupling in coherent fibre bundles

Helen E. Parker, Antonios Perperidis, Ahmed Karam-Eldaly, Yoann Altmann, Kevin Dhaliwal, et al.

Helen E. Parker, Antonios Perperidis, Ahmed Karam-Eldaly, Yoann Altmann, Kevin Dhaliwal, Robert R. Thomson, Stephen McLaughlin, Michael G. Tanner, "Characterising cross-coupling in coherent fibre bundles," Proc. SPIE 11076, Advances in Microscopic Imaging II, 110761D (22 July 2019); doi: 10.1117/12.2527054

SPIE.

Event: European Conferences on Biomedical Optics, 2019, Munich, Germany

Characterising Cross-Coupling in Coherent Fibre Bundles

Helen E. Parker[a], Antonios Perperidis[a,b], Ahmed Karam-Eldaly[b], Yoann Altmann[b], Kevin Dhaliwal[a], Robert R. Thomson[a,c], Stephen McLaughlin[b], and Michael G. Tanner[a,c]

[a]EPSRC Proteus IRC Hub, Centre for Inflammation Research, Queens Medical Research Institute, University of Edinburgh, UK
[b]Institute of Sensors, Signals and Systems (ISSS), Heriot Watt University, UK
[c]Institute of Photonics and Quantum Sciences (IPAQS), Heriot Watt University, UK

ABSTRACT

Fibre-bundle endomicroscopy is an emerging medical imaging tool. Inter-core coupling within coherent fibre bundles limits the technology's imaging capabilities. We introduce a novel approach for quantifying and modelling cross coupling, optimising image reconstruction.

1. INTRODUCTION

Fibre-bundle endomicroscopy[1] (FBEμ) is an emerging, fibre-based imaging tool with clinical and pre-clinical utility. FBEμ has been deployed to image a range of organ systems, including the gastro-intestinal,[2] urological[3] and the respiratory tracts.[4] Recent developments in FBEμ and associated fluorescent SmartProbes present a need for sensitive imaging with high detection performance.[5] Inter-core coupling within coherent fibre bundles is a well recognised limitation, resulting in blurring of the imaged structures and consequently a worsening in the associated limits of detection. Fibre cross coupling has been studied both experimentally[6] and within a theoretical framework (coupled mode theory),[7] providing recommendations for optimal fibre bundle design. However, due to physical limitations, such as the trade-off between cross coupling and core density, cross coupling can be suppressed yet not eliminated through optimal fibre design. This study introduces a novel approach for measuring, analysing and quantifying cross coupling within coherent fibre bundles, in a format that can be integrated into a linear model, which in turn can enable computational compensation of the associated blurring introduced to FBEμ images. More details can be found in.[8,9]

2. METHODOLOGY

Multiple (12) regions-of-interest (ROIs) consisting of 25 neighbouring cores, each in a rectangular arrangement, were measured at 520 nm and 635 nm. Prior to the acquisition of each ROI, a flood illumination image of the fibre was captured with a CMOS camera(Fig. 1.a), (i) ensuring that the imaging system was in focus at the camera end of the fibre, (ii) enabling the segmentation of the individual cores within the field-of-view, (iii) extracting their associated size and location parameters (Fig. 1.b), and (iv) creating a connectivity list between cores, identifying r^{th} -order neighbours ($r = [1, 5]$) for each measured core (Fig. 1.c). Then, for each individually illuminated (laser) core within a ROI, an image at the distal end of the fibre was acquired, enabling the quantification of the light coupled through the central core as well as its immediate and extended neighbours (Fig. 2). The optimal position of the incident laser light was manually adjusted, illuminating the centre of the examined core. Finally, for each image within a 25-core ROI, the mean intensity across pixels in the binary mask associated with the central core, as well as each of the r^{th}-order neighbouring cores, was estimated and distributions of the associated coupling spreads were derived. This information was used to create a forward linear model $v = Hu + \omega$ of the average light cross coupling across a coherent fibre bundle. H was the matrix representation of a convolutional operator modelling average cross coupling between fibre cores. Vector ω represented the additive Gaussian noise.

Further author information: (Send correspondence to H.E.P.: E-mail: h.parker@ed.ac.uk)

Advances in Microscopic Imaging II, edited by Emmanuel Beaurepaire, Francesco Saverio Pavone
Proc. of SPIE-OSA Vol. 11076, 110761D · © 2019 SPIE-OSA · CCC
code: 1605-7422/19/$21 · doi: 10.1117/12.2527054

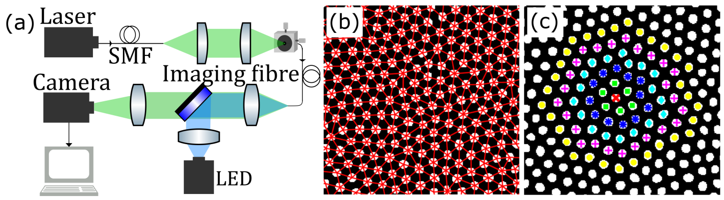

Figure 1. (a) System for illuminating (635 nm and 520 nm) a single core within a coherent fibre bundle, and recording the coupling of light across its neighbours. Example binary mask highlighting cores and the associated (b) triangulation, linking cores to (c) immediate & extended neighbours. Images (a) and (b-c) have been reproduced (cropped) from Figures 1 and 7 respectively of *Characterization and modelling of inter-core coupling in coherent fiber bundles* by (Perperidis et al., 2017b) under CC BY 4.0.

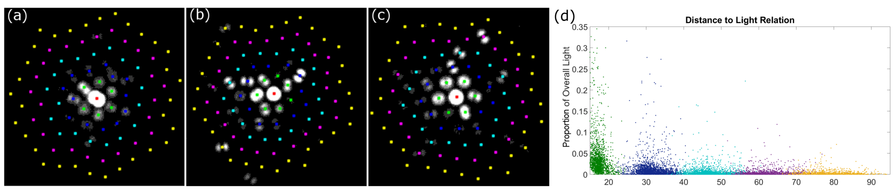

Figure 2. Broad coupling pattern categories: (a) even spread fading with distance, (b) seemingly random spread in both location and magnitude, and (c) a combination of the even and random spreads. (d) Distance (in pixels) of each core to the corresponding central core against the proportion of light coupled through the core at 635 nm. Cores grouped into neighbouring layers from immediate (green) to extended (blue, cyan, magenta, yellow) Images (a-c) and (d) have been reproduced (cropped) from Figures 8 and 11 respectively of *Characterization and modelling of inter-core coupling in coherent fiber bundles* by (Perperidis et al., 2017b) under CC BY 4.0.

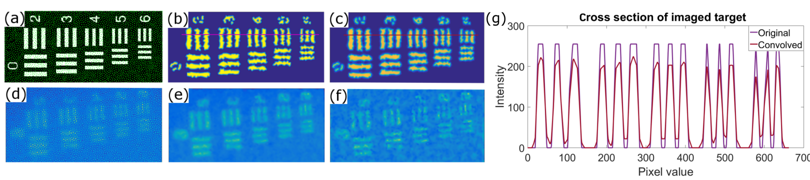

Figure 3. Cross coupling effect on simulated (a-c) and real (d-f) FBEμ images of the USAF chart. (a) Binary image of USAF chart, fibre-core locations, (b) interpolation, (c) image after applying estimated cross coupling. (d) Real FBEμ image of fluorescent USAF chart. (e) Interpolated image. (f) Processed image estimating the original de-convolved data.[9] (g) Cross section of image target. Images (a-f) and (g) have been reproduced (cropped) from Figure 15 and 16, respectively of *Characterization and modelling of inter-core coupling in coherent fiber bundles* by (Perperidis et al., 2017b) under CC BY 4.0.

3. RESULTS AND DISCUSSION

Figure 2 demonstrates characteristic coupling spreads from the central core, broadly categorised into three classes, (a) relative even spread amongst neighbours, fading with distance, (b) seemingly random spread in both location and magnitude, and (c) a combination of the even spread implanted with random cores of high coupling. The exact coupling pattern for an individual core can be affected by movement of the fibre bundle. Consequently, quantifying the overall spread of light to neighbouring core layers provides a more robust statistical characterisation. Fig. 2.d illustrates the relationship of the proportion of light coupled to a core, and its distance to the central (illuminated) core at 635 nm. While overall coupling tends to decrease with distance from the central core, when observed in terms of individual neighbouring layers there appears to be no direct correlation between small distance changes and relevant light coupling changes. Similar behaviour is observed at 520 nm. Subsequent analysis was based on grouping cores into 5 neighbouring layers rather than explicitly considering the distance of a core to the illuminated central core. Table 1 summarises the underlying distributions of the spread of light to neighbouring layers. To assess the effect of the estimated light cross coupling, simulated data, as imaged through a coherent fibre bundle, of a USAF 1951 chart were generated (Fig. 3.a-c). In addition, real FBEμ images of the USAF chart were recorded, prior to any sampling/interpolation (Fig. 3.d) and after linear interpolation removing the core honeycomb patterns (Fig. 3.e). The proposed model (Fig. 3.c) provides a close match to the substantial image degradation observed in real FBEμ data (Fig. 3.e). Applying an optimisation based deconvolution and restoration method can remove the effect of cross coupling increasing the contrast (Fig. 3.f).

4. CONCLUSIONS

This study demonstrated the feasibility of a robust distribution estimation of cross coupling spread at 520 nm and 635 nm. The quantified coupling spread can be fed into a linear model, which in turn can be employed to computationally estimate the underlying, de-coupled data. Future directions include characterising a range of coherent fibre bundles, and developing novel algorithms to computationally compensate for inter-core coupling.

Table 1. Mean coupling spread per individual core as well as per neighbouring layer.

	520 nm		635 nm	
Layer	Mean per core (SD)	Mean per layer	Mean per core (SD)	Mean per layer
Central	61.0 (9.1)	61.0	61.7 (13.6)	61.7
1^{st}	5.6 (4.7)	33.6	3.8 (4.5)	22.7
2^{st}	3.1 (1.2)	3.8	0.7 (1.9)	8.9
3^{rd}	0.1 (0.4)	1.1	0.2 (0.8)	3.6
4^{th}	0.0 (0.2)	0.4	0.1 (0.4)	2.0
5^{th}	0.0 (0.1)	0.2	0.0 (0.2)	1.1

ACKNOWLEDGMENTS

This work has been funded by the Engineering and Physical Sciences Research Council (EPSRC, United Kingdom) (EP/K03197X/1). We would also like to thank Kerrianne Harrington for the fibre-bundle SEM images.

REFERENCES

[1] Perperidis, A., Dhaliwal, K., McLaughlin, S., and Vercauteren, T., "Image computing for fibre-bundle endomicroscopy: A review," *CoRR* **abs/1809.00604** (2018).

[2] Wallace, M. B. and Fockens, P., "Probe-Based Confocal Laser Endomicroscopy," *Gastroenterology* **136**(5), 1509–1513 (2009).

[3] Pan, Y., Volkmer, J.-P., Mach, K. E., Rouse, R. V., Liu, J.-J., Sahoo, D., Chang, T. C., Metzner, T. J., Kang, L., van de Rijn, M., Skinner, E. C., Gambhir, S. S., Weissman, I. L., and Liao, J. C., "Endoscopic molecular imaging of human bladder cancer using a CD47 antibody," *Science Translational Medicine* **6**, 260ra148–260ra148 (oct 2014).

[4] Thiberville, L., Moreno-Swirc, S., Vercauteren, T., Peltier, E., Cavé, C., and Bourg Heckly, G., "In Vivo Imaging of the Bronchial Wall Microstructure Using Fibered Confocal Fluorescence Microscopy," *American Journal of Respiratory and Critical Care Medicine* **175**, 22–31 (jan 2007).

[5] Eldaly, A. K., Altmann, Y., Akram, A. R., Perperidis, A., Dhaliwal, K., and McLaughlin, S., "Patch-based sparse representation for bacterial detection," *CoRR* **abs/1810.12043** (2018).

[6] Wood, H. A. C., Harrington, K., Stone, J. M., Birks, T. A., and Knight, J. C., "Quantitative characterization of endoscopic imaging fibers," *Optics Express* **25**, 1985 (feb 2017).

[7] Reichenbach, K. L. and Xu, C., "Numerical analysis of light propagation in image fibers or coherent fiber bundles," *Optics Express* **15**(5), 2151 (2007).

[8] Perperidis, A., Parker, H. E., Karam-Eldaly, A., Altmann, Y., Dhaliwal, K., Thomson, R. R., Tanner, M. G., and McLaughlin, S., "Characterization and modelling of inter-core coupling in coherent fiber bundles," *Optics Express* (2017).

[9] Eldaly, A. K., Altmann, Y., Perperidis, A., Krstajic, N., Choudhary, T., Dhaliwal, K., and McLaughlin, S., "Deconvolution and restoration of optical endomicroscopy images," *CoRR* **abs/1701.08107** (2017).